Supplementary Material

Highly Stereoregular 1,3-Butadiene and Isoprene Polymers through Monoalkyl− *N*−aryl Substituted Iminopyridine Iron Complexes-based Catalysts: Synthesis and Characterization

Giovanni Ricci,[a,*] Giuseppe Leone,[a] Giorgia Zanchin,[a] Benedetta Palucci,[a] Antonella Caterina Boccia,[a] Anna Sommazzi,[b] Francesco Masi,[c] Stefano Zacchini,[d] Massimo Guelfi,[e] and Guido Pampaloni[e]

[a] CNR-Istituto di Scienze e Tecnologie Chimiche "Giulio Natta" (SCITEC), via A. Corti 12, I-20133 Milano, Italy.

[b] Versalis S.p.A. - Centro Ricerca Novara – Via G. Fauser 4, I-28100 Novara (NO), Italy.

[c] Versalis S.p.A. - R&D Partner Catalysis – Piazza Boldrini 1, I-20097 San Donato Milanese (MI), Italy.

[d] Università di Bologna, Dipartimento di Chimica Industriale ''Toso Montanari'', Viale Risorgimento 4, I-40136 Bologna, Italy.

[e] Università di Pisa, Dipartimento di Chimica e Chimica Industriale, Via Moruzzi 13, I-56124 Pisa, Italy.

Figures S1−S8. FT-IR spectra of iron complexes.

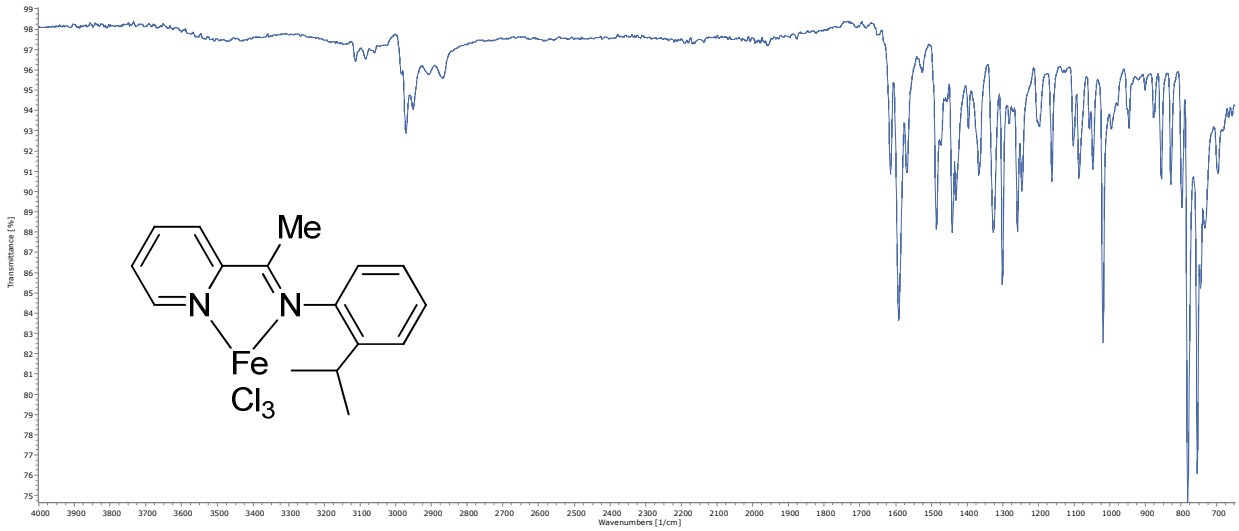

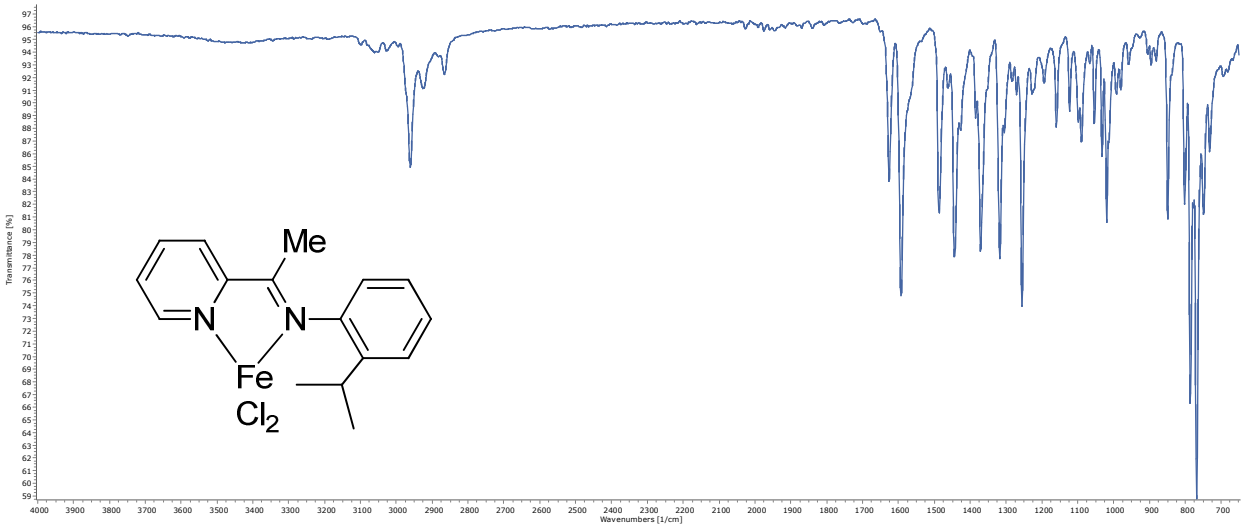

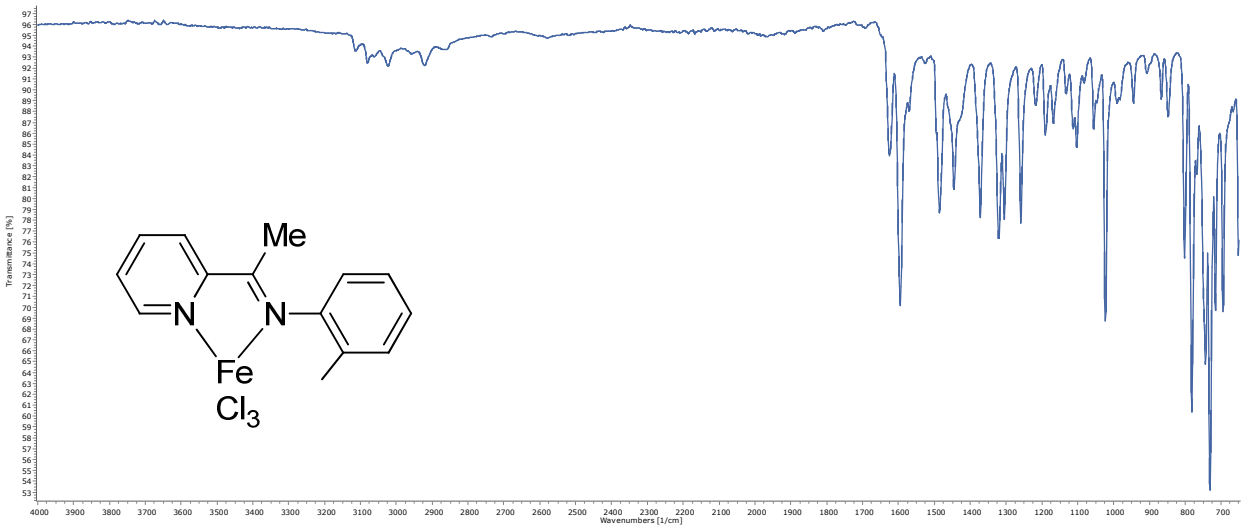

Me
N
N
Fe
Cl2
Transmittance [%]
Wavenumbers [1/cm]

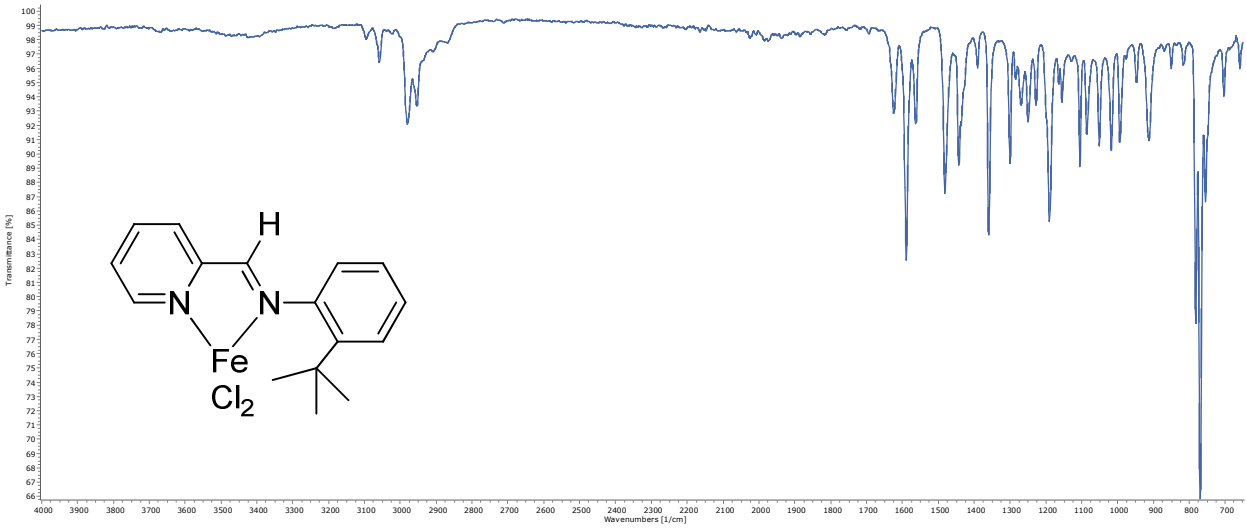
H
N
N
Fe
Cl2
Transmittance [%]
Wavenumbers [1/cm]

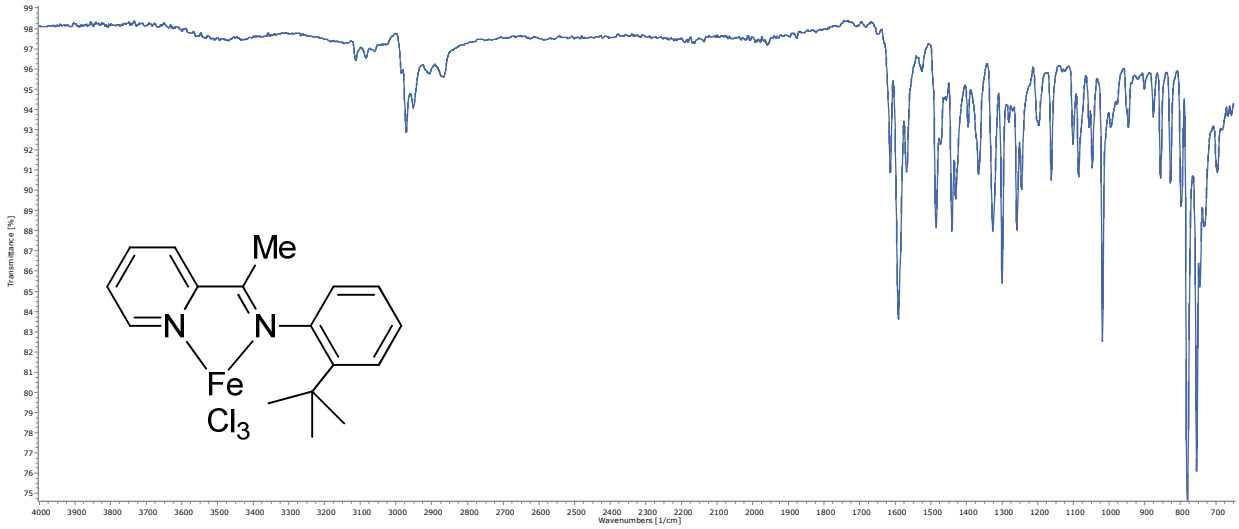
Me
N
N
Fe
Cl3
Transmittance [%]
Wavenumbers [1/cm]

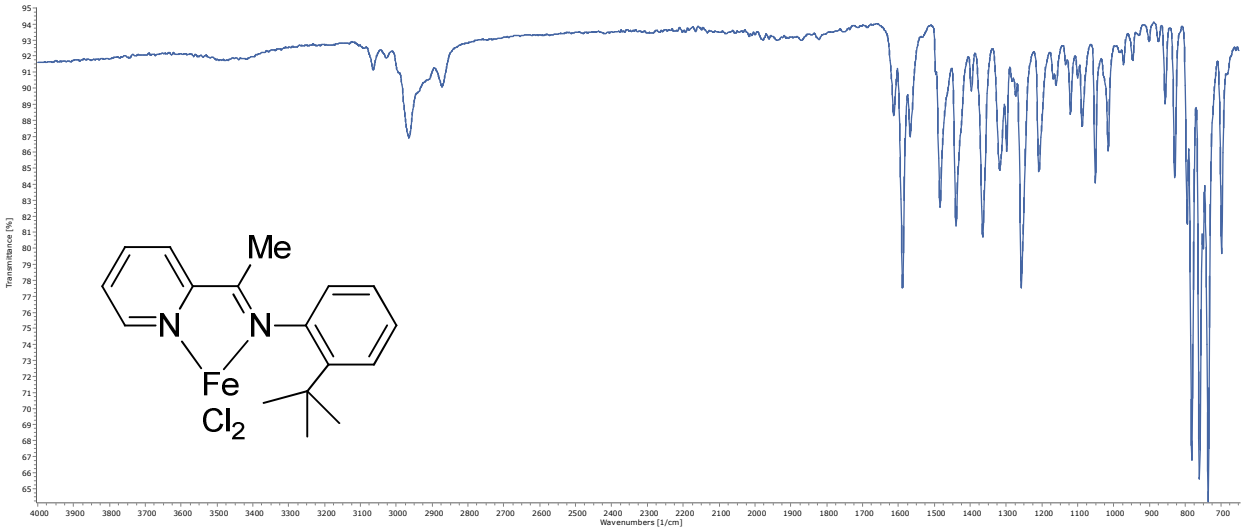
Me
N
N
Fe
Cl2
Transmittance [%]
Wavenumbers [1/cm]

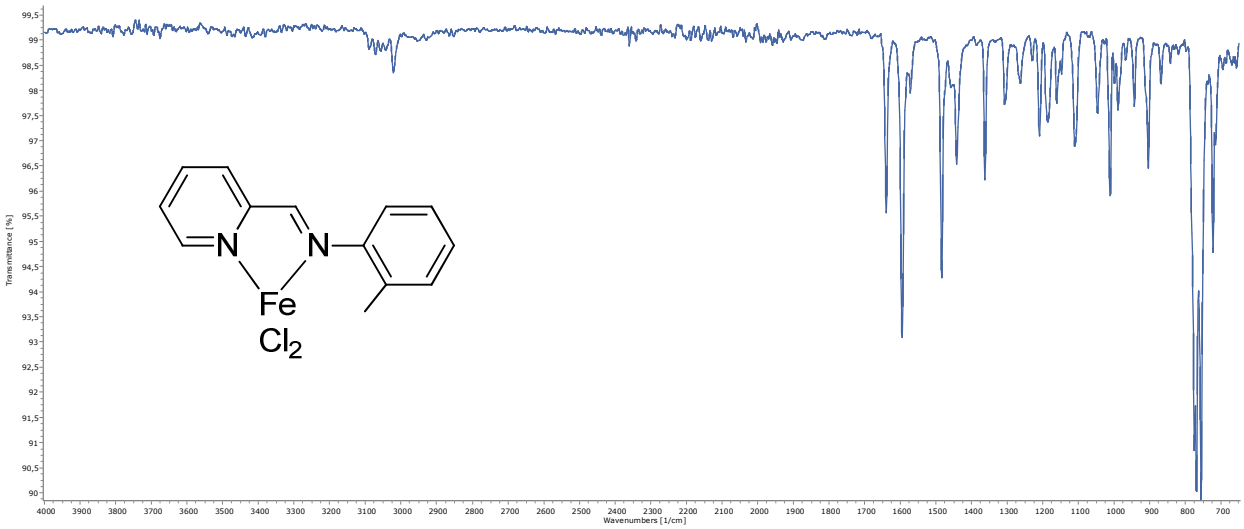
N
N
Fe
Cl2
Transmittance [%]
Wavenumbers [1/cm]

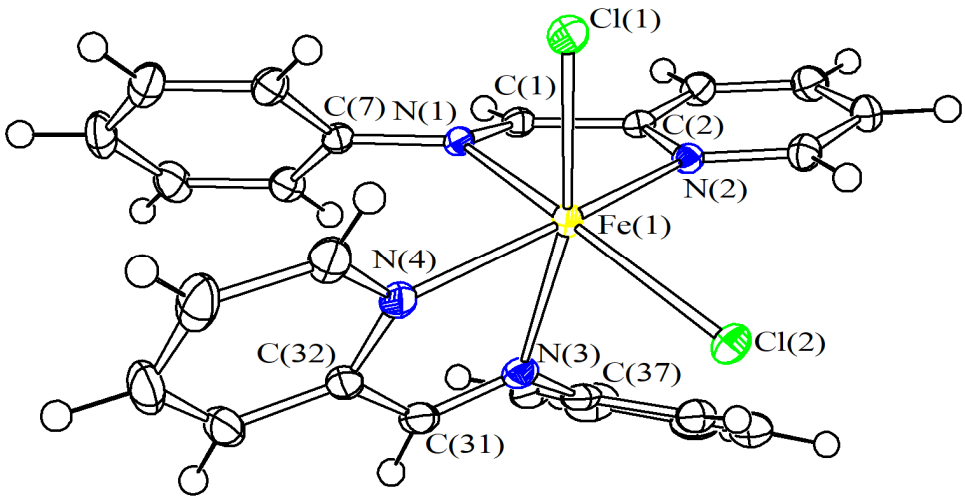

Figure S9. Molecular structure of **Fe2-L6·MeOH**, with key atoms labeled. Displacement ellipsoids are at the 50% probability level.

Table S1. Selection of bond distances (Å) and angles (deg) for **Fe2-L6·MeOH**.

Fe(1)-Cl(1)	2.3544(4)	Fe(1)-Cl(2)	2.4432(4)
Fe(1)-N(1)	2.2897(12)	Fe(1)-N(2)	2.1714(12)
Fe(1)-N(3)	2.2512(13)	Fe(1)-N(4)	2.1686(13)
N(1)-C(1)	1.2788(19)	N(3)-C(31)	1.279(2)
N(1)-C(7)	1.4234(18)	N(3)-C(37)	1.427(2)
C(1)-C(2)	1.464(2)	C(31)-C(32)	1.464(3)
N(2)-C(2)	1.3502(19)	N(4)-C(32)	1.353(2)
Cl(1)-Fe(1)-Cl(2)	97.990(14)	N(1)-Fe(1)-N(2)	73.49(4)
N(3)-Fe(1)-N(4)	74.11(5)	Cl(1)-Fe(1)-N(3)	166.13(4)
Cl(2)-Fe(1)-N(1)	162.40(3)	N(2)-Fe(1)-N(4)	160.02(5)
Fe(1)-N(1)-C(1)	113.58(10)	Fe(1)-N(3)-C(31)	114.24(11)
C(7)-N(1)-C(1)	119.41(12)	C(37)-N(3)-C(31)	120.58(14)
N(1)-C(1)-C(2)	118.67(13)	N(3)-C(31)-C(32)	118.71(15)
C(1)-C(2)-N(2)	115.79(13)	C(31)-C(32)-N(4)	115.53(14)
C(2)-N(2)-Fe(1)	116.95(10)	C(32)-N(4)-Fe(1)	115.71(11)

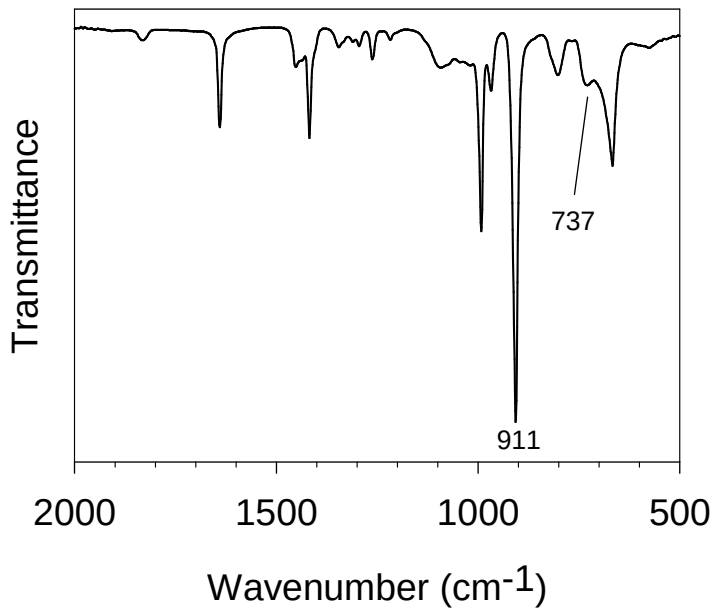

Figure S10. FT-IR spectrum of entry 2, Table 5.

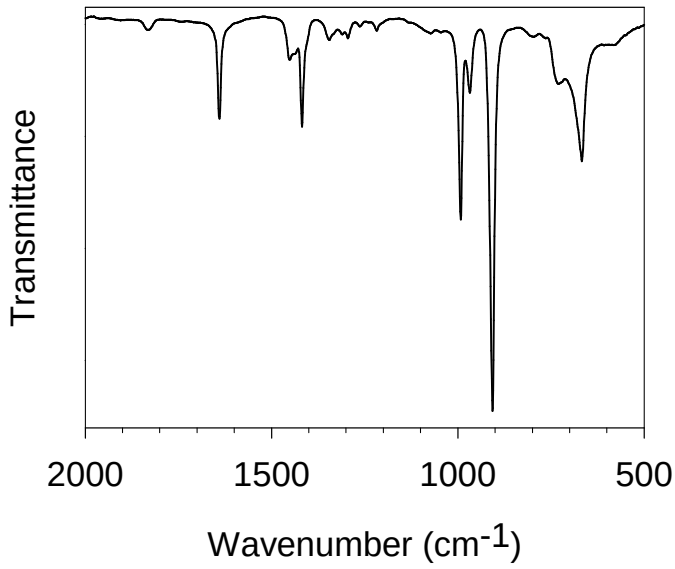

Figure S11. FT-IR spectrum of entry 3, Table 5.

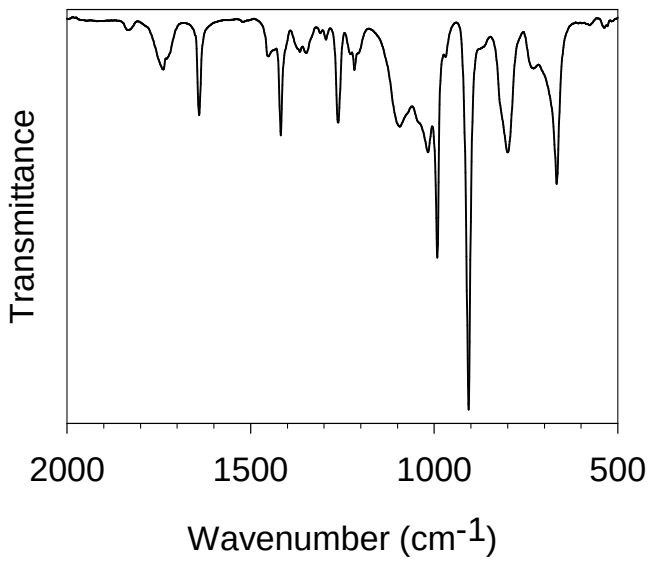

Figure S12. FT-IR spectrum of entry 4, Table 5

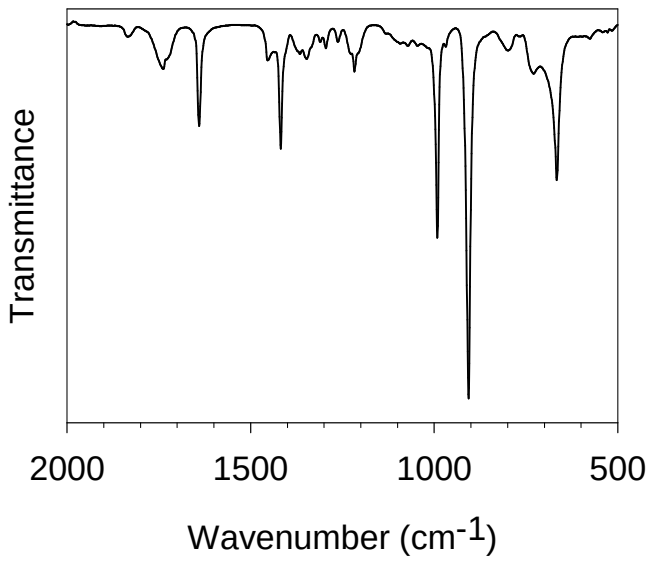

Figure S13. FT-IR spectrum of entry 5, Table 5

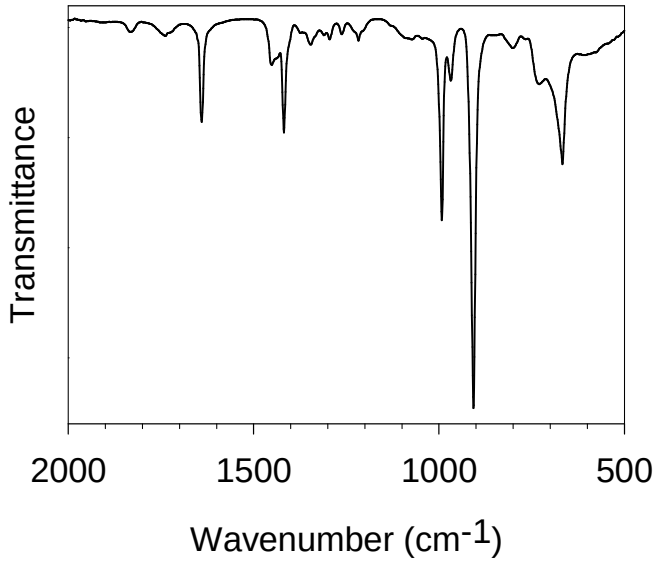

Figure S14. FT-IR spectrum of entry 6, Table 5

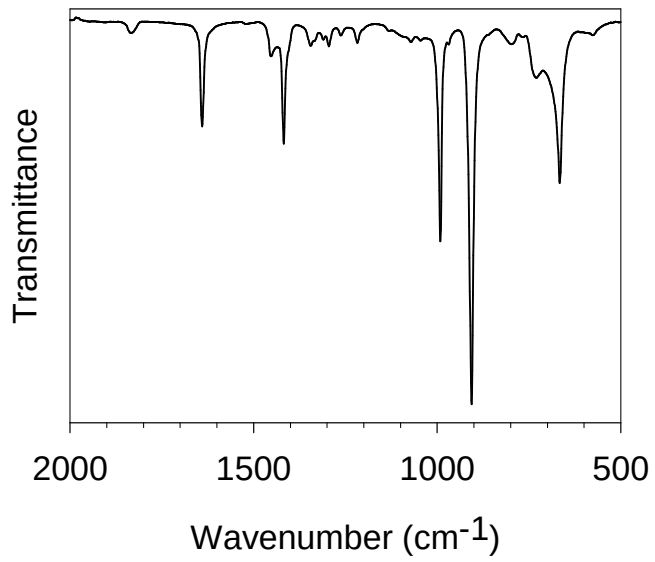

Figure S15. FT-IR spectrum of entry 7, Table 5

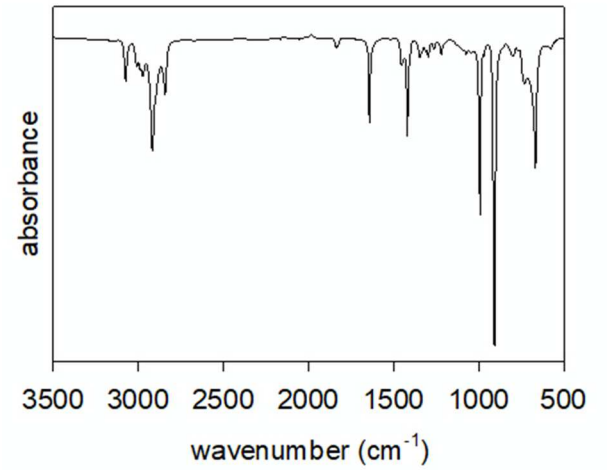

Figure S16. FT-IR spectrum of entry 8, Table 5

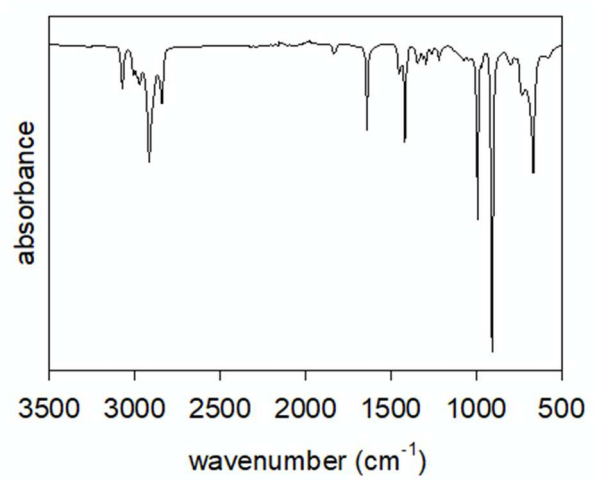

Figure S17. FT-IR spectrum of entry 9, Table 5

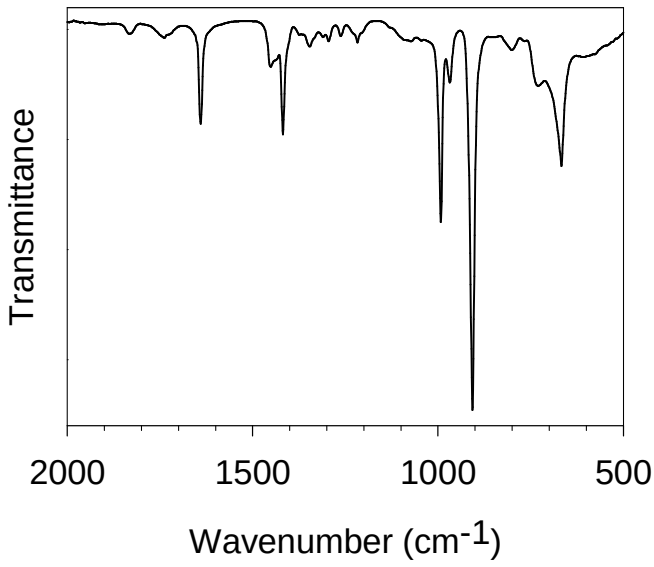

Figure S18. FT-IR spectrum of entry 10, Table 5

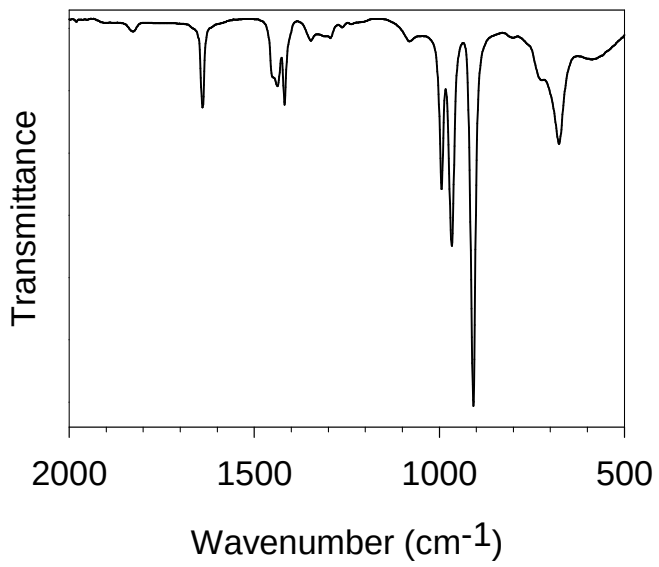

Figure S19. FT-IR spectrum of entry 12, Table 5

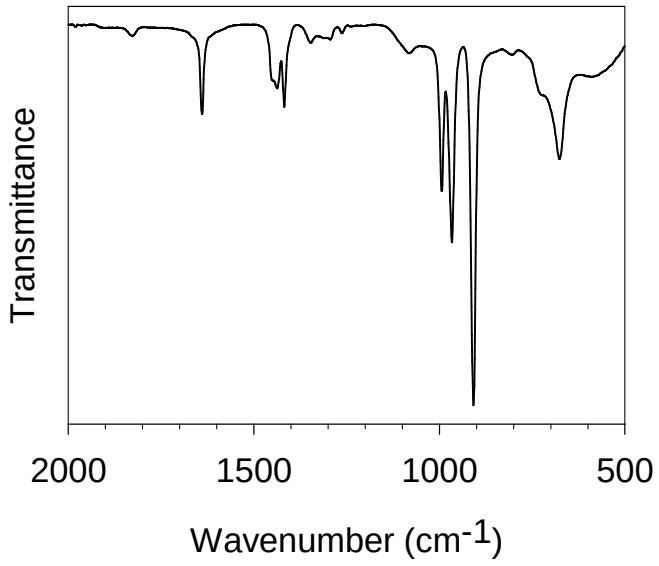

Figure S20. FT-IR spectrum of entry 13, Table 5

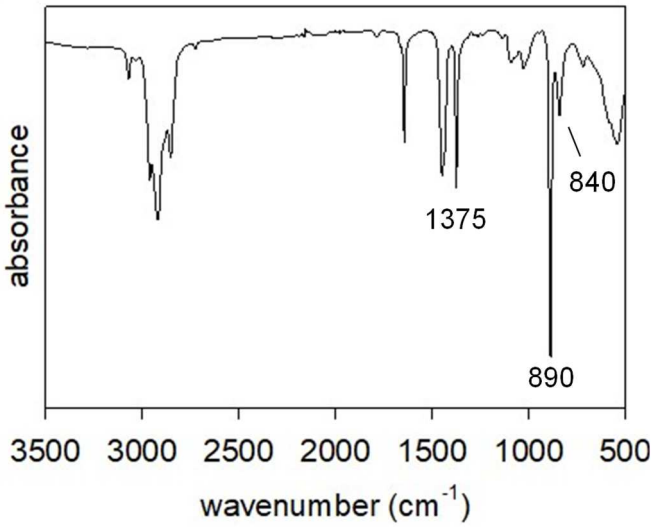

Figure S21. FT-IR spectrum of entry 14, Table 6

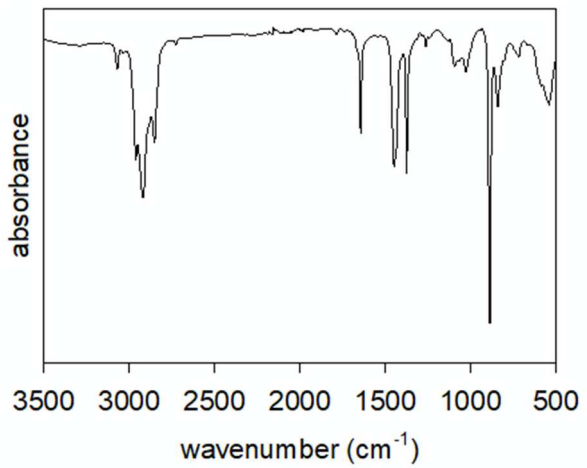

Figure S22. FT-IR spectrum of entry 15, Table 6

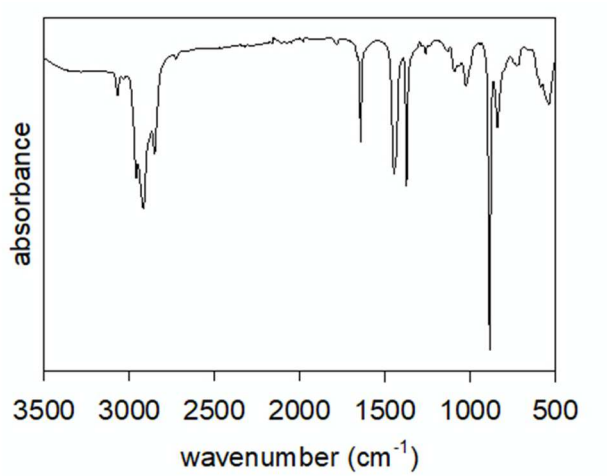

Figure S23. FT-IR spectrum of entry 16, Table 6

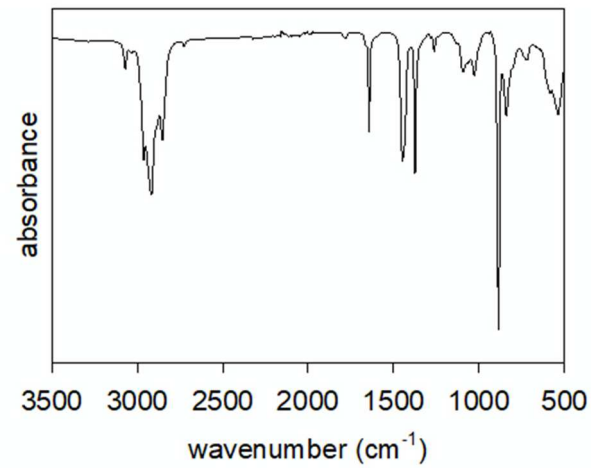

Figure S24. FT-IR spectrum of entry 17, Table 6

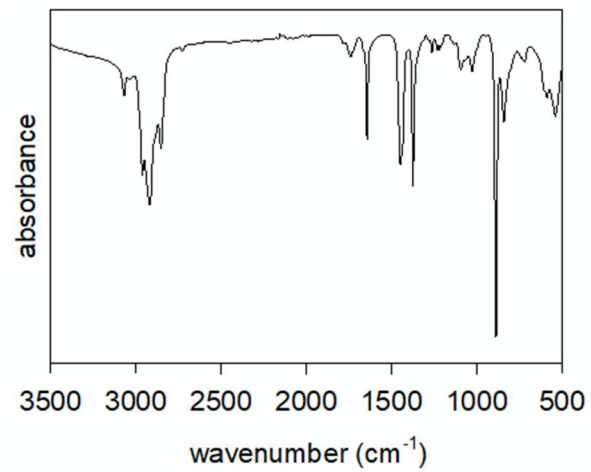

Figure S25. FT-IR spectrum of entry 18, Table 6

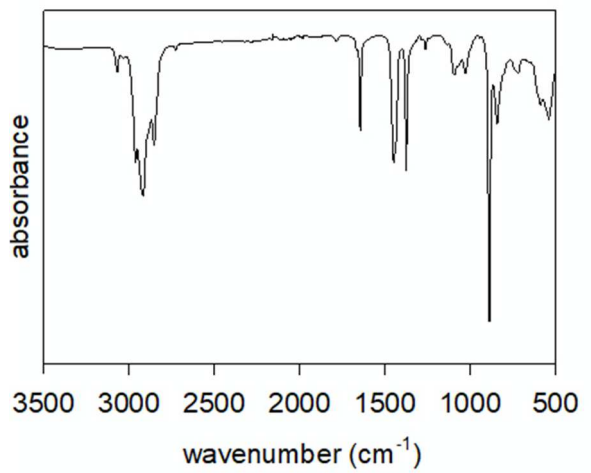

Figure S26. FT-IR spectrum of entry 19, Table 6

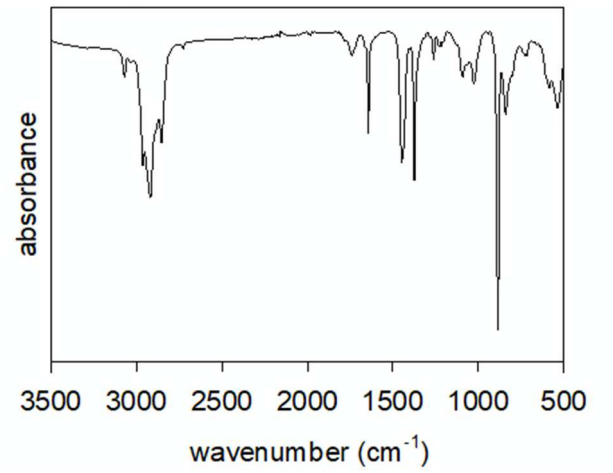

Figure S27. FT-IR spectrum of entry 20, Table 6

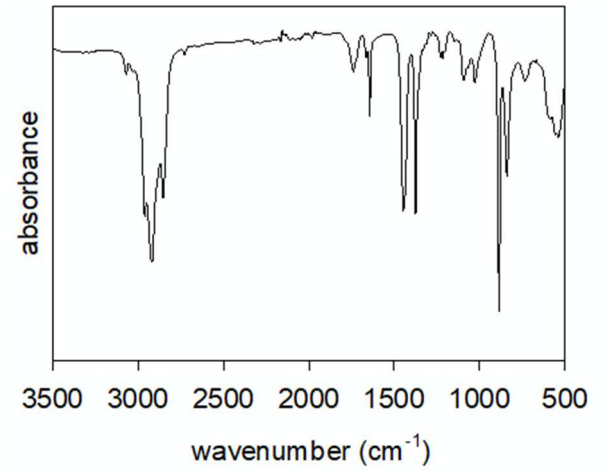

Figure S28. FT-IR spectrum of entry 21, Table 6

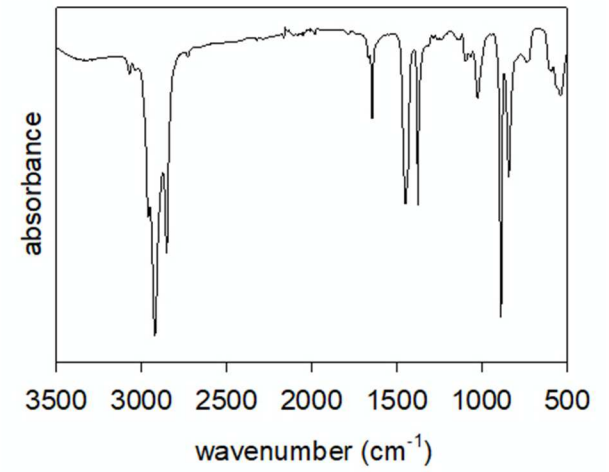

Figure S29. FT-IR spectrum of entry 24, Table 6

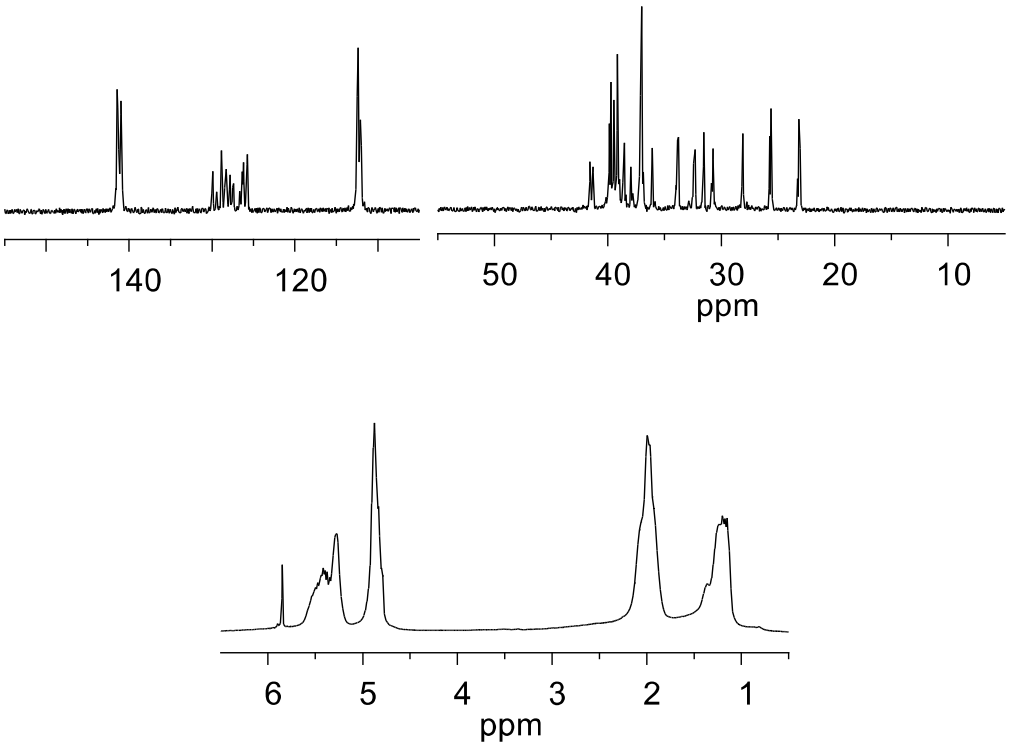

Figure S30. ^{13}C (top) and ^{1}H (down) NMR spectra of entry 1, Table 5

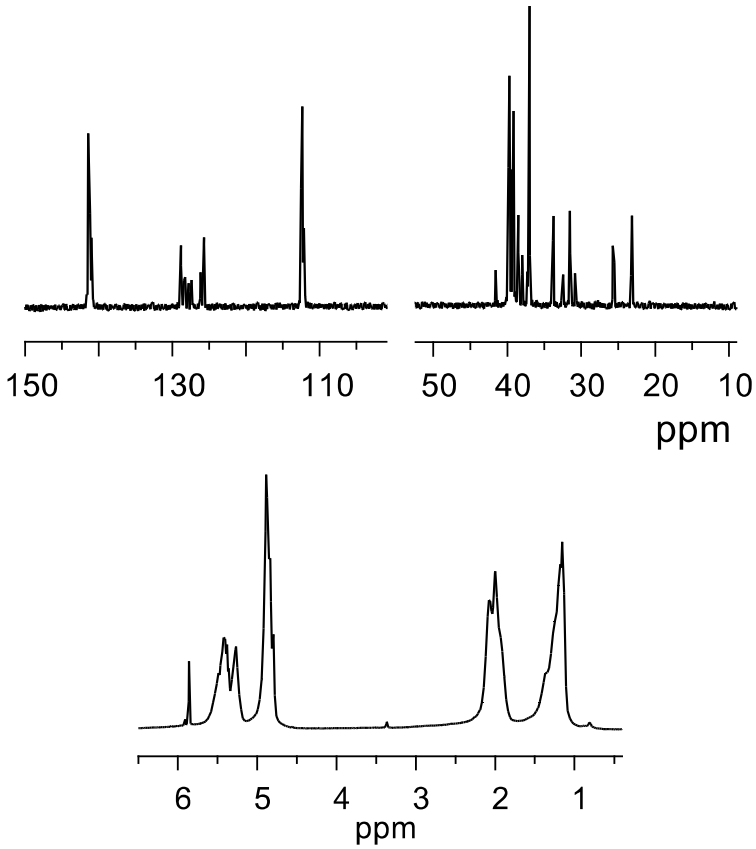

Figure S31. ^{13}C (top) and ^{1}H (down) NMR spectra of entry 9, Table 5

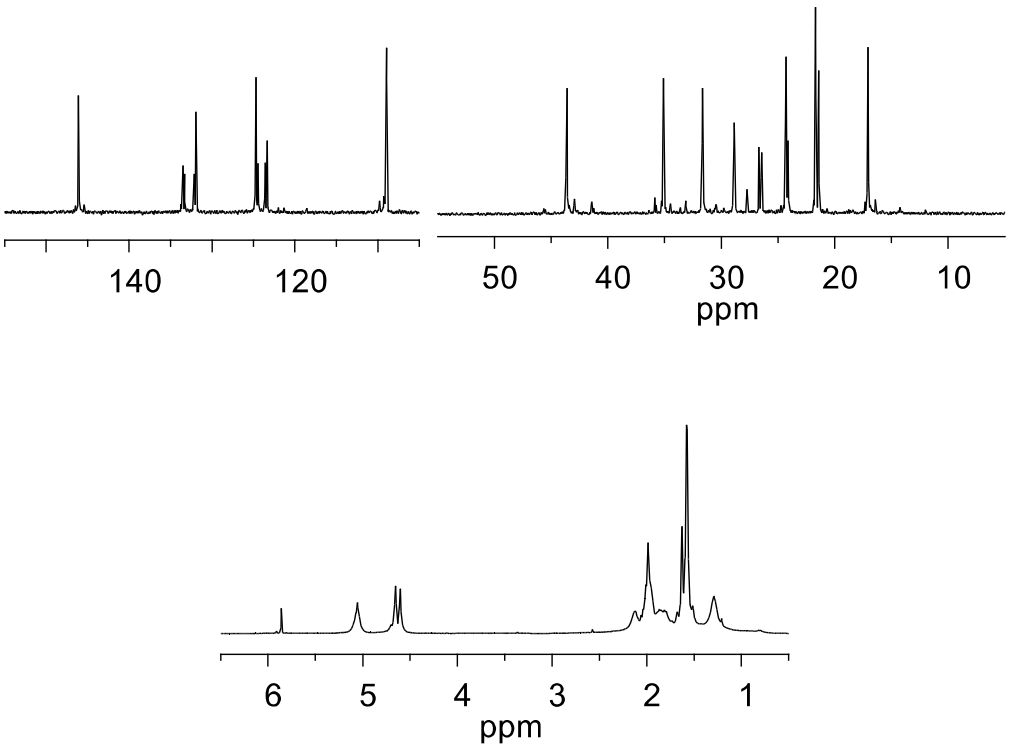

Figure S32. ^{13}C (top) and ^{1}H (down) NMR spectra of entry 19, Table 6

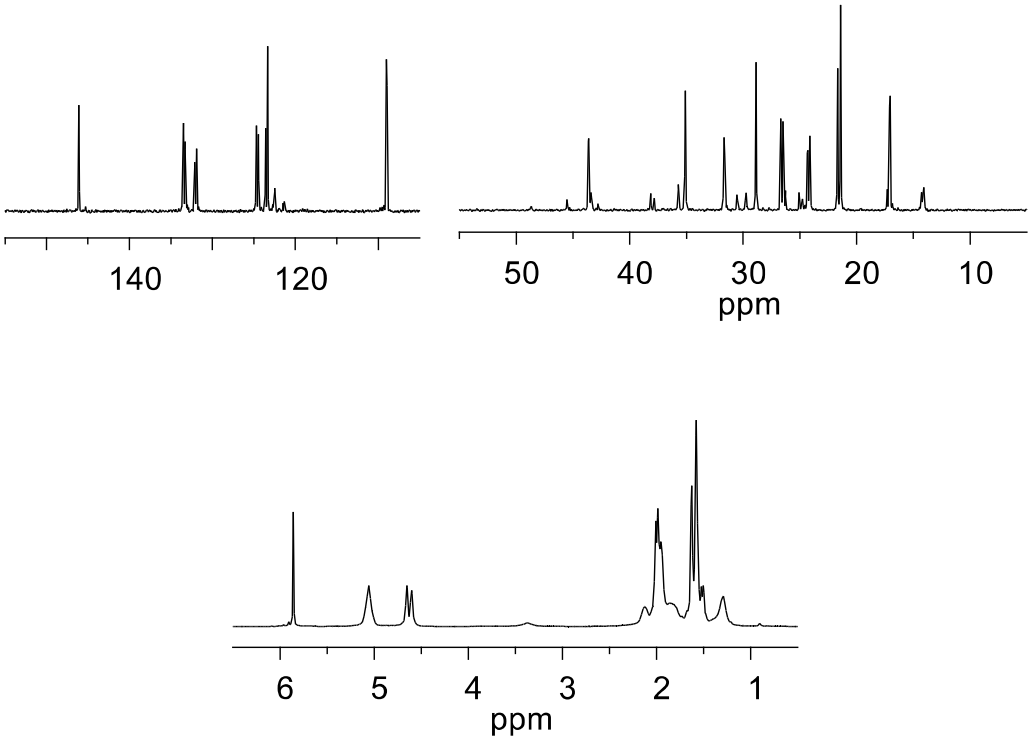

Figure S33. ^{13}C (top) and ^{1}H (down) NMR spectra of entry 24, Table 6

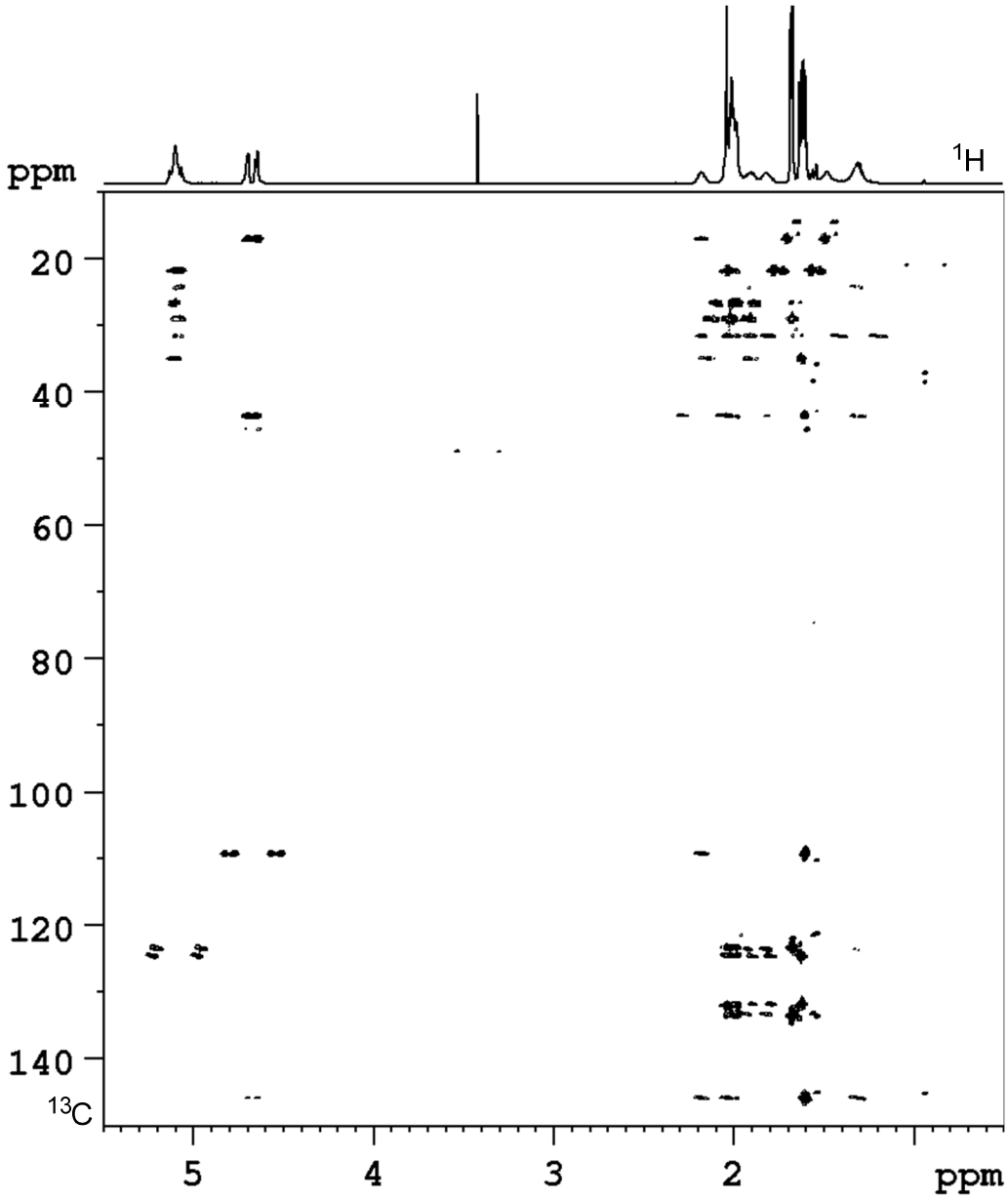

Figure S34. ^{1}H-^{13}C HMBC spectrum of entry 22 of Table 6, recorded at 330K in *d*TCE.

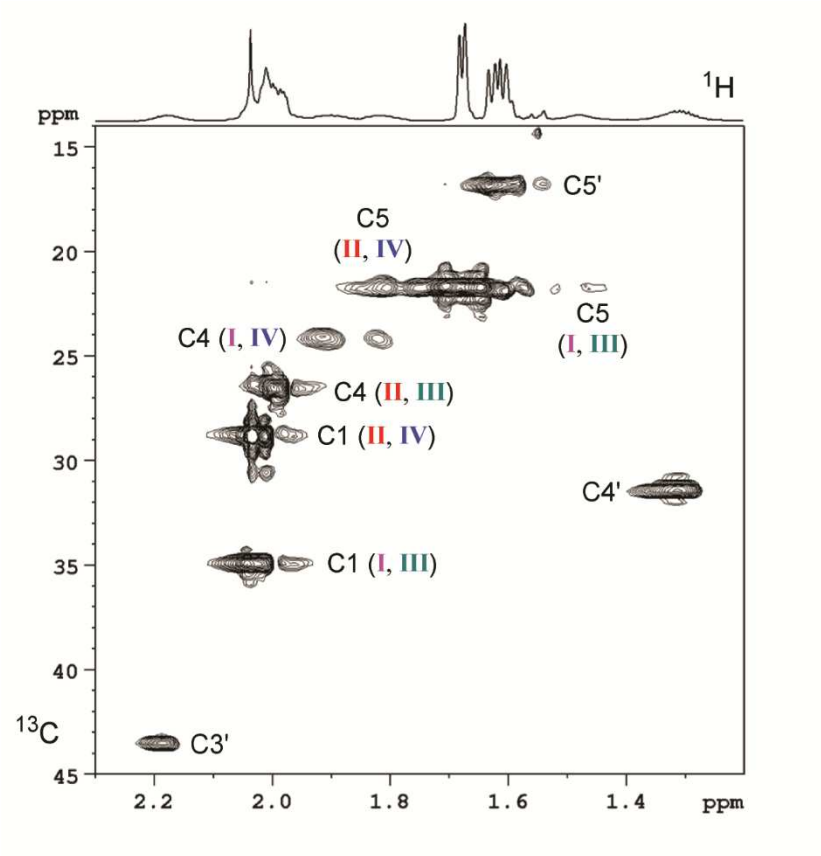

Figure S35. Aliphatic region of ^{1}H-^{13}C HSQC spectrum of entry 22 of Table 6, recorded at 330K in *d*TCE.

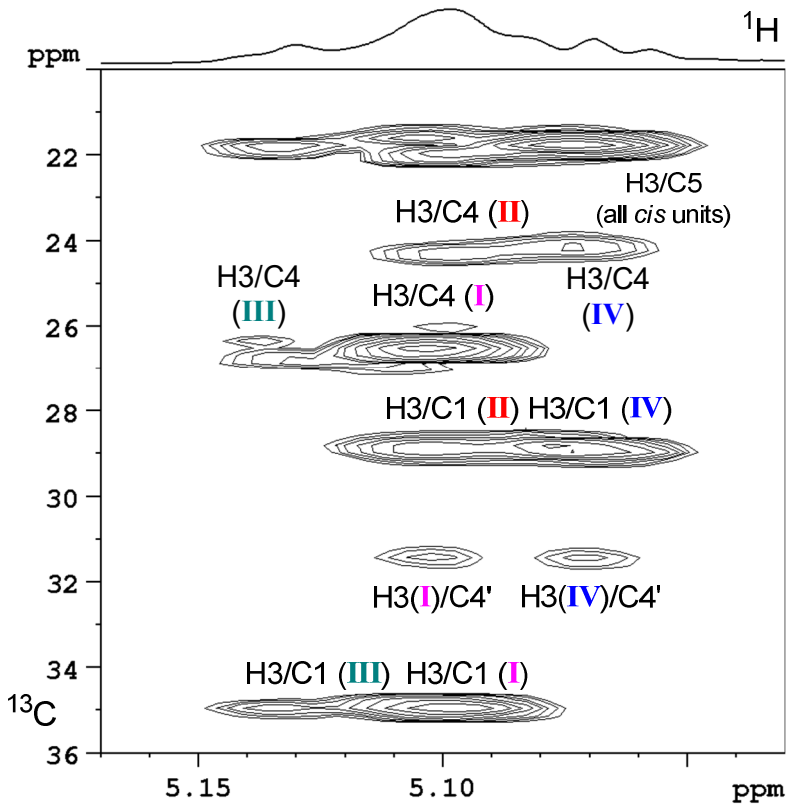

Figure S36. Expanded region of ^{1}H-^{13}C HMBC spectrum of entry 22 of Table 6, recorded at 330K in *d*TCE.